SAND2014-20148PE

Design, Fabrication, and Characterization of High Density Silicon Photonic Components

Adam M. Jones

November 18, 2014

Sandia National Laboratories is a multi-program laboratory managed and operated by Sandia Corporation, a wholly owned subsidiary of Lockheed Martin Corporation, for the U.S. Department of Energy's National Nuclear Security Administration under contract DE-AC04-94AL85000.

Notes

1. Link at bottom to supplementary slide w/links to all slides
2. Footer with page number, Sandia logo and OpSci logo
3. Section in footer, lower left
4. In RLP section, change \alpha_{TOT} to \alpha_{DUT}
5. Make all fonts same, choose one w/o fine features
6. Make sure each slide highlights bottom line
7. SiPh slide – focus on CMOS 7, III-V integration, group IV photonics,
8. Show TE only, but say so
9. Add intro/conclusion slides to each section
10. Remove curve fitting slides
11. Add 'other work' slide
12. NOS – other 3D approaches, mention modification of crossing geometry as future work
13. Xmode - Note FDTD, add schematic, explain units, power input, wavelength
14. XT – importance of geometric mean
15. Synchronize gap/interlayer thickness verbage
16. XS – measurement difficulties & how data presented.
17. IPLM – rename 'Loss Measurement Overview', distinguish/describe two kinds of loss.
18. RLPCal – add image showing inserted structure loss estimation
19. RLPref – note corresponence to taper length rather than taper length (plot legend)
20. SPKtrans – make result jump out

Data Demands

Teleconferencing • Web Browsing • Video/Music streaming • Data storage

VoIP • Electronic health records • Web conferencing

Virtual office • Telemedicine • Cloud-based learning

Pop. Pen.

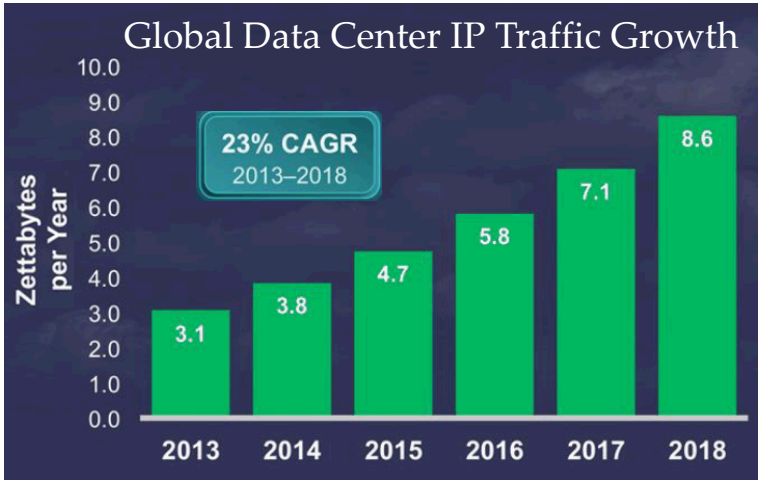

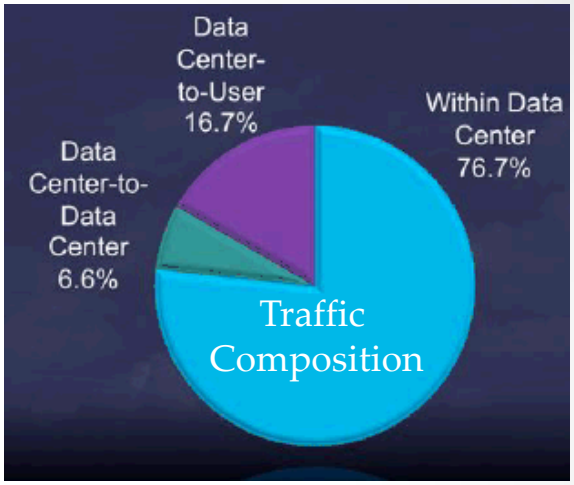

- Petaflop machines require 5 to 10MW of power to operate with ~25% of that devoted to the computer network.
- Exaflop machines could require GW of power to operate.
- The Palo Verde Nuclear Generation Site generates 3.3GW.
- Photonic devices could reduce power requirements by two orders of magnitude compared to electronic components.
- This would bring Exaflop machine power requirements back to the MW regime.

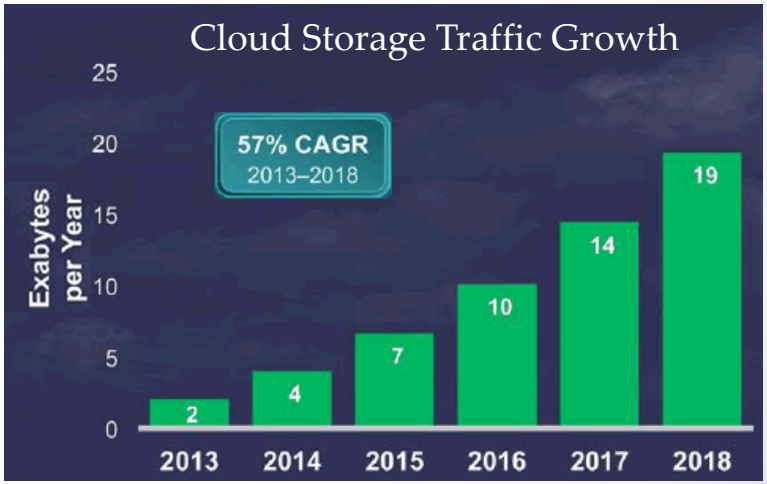

Connected vehicle safety applications • High frequency stock trading • Email/IM

High Performance Computers & Data Center Networks

- Data center comprised of multiple racks of multiple blade servers all of which are network connected.
- 75% of total traffic is within the data center.

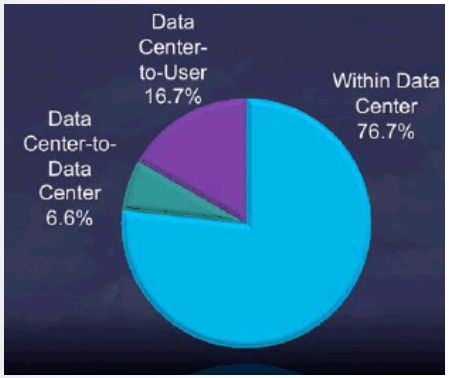

HPC / Data Center

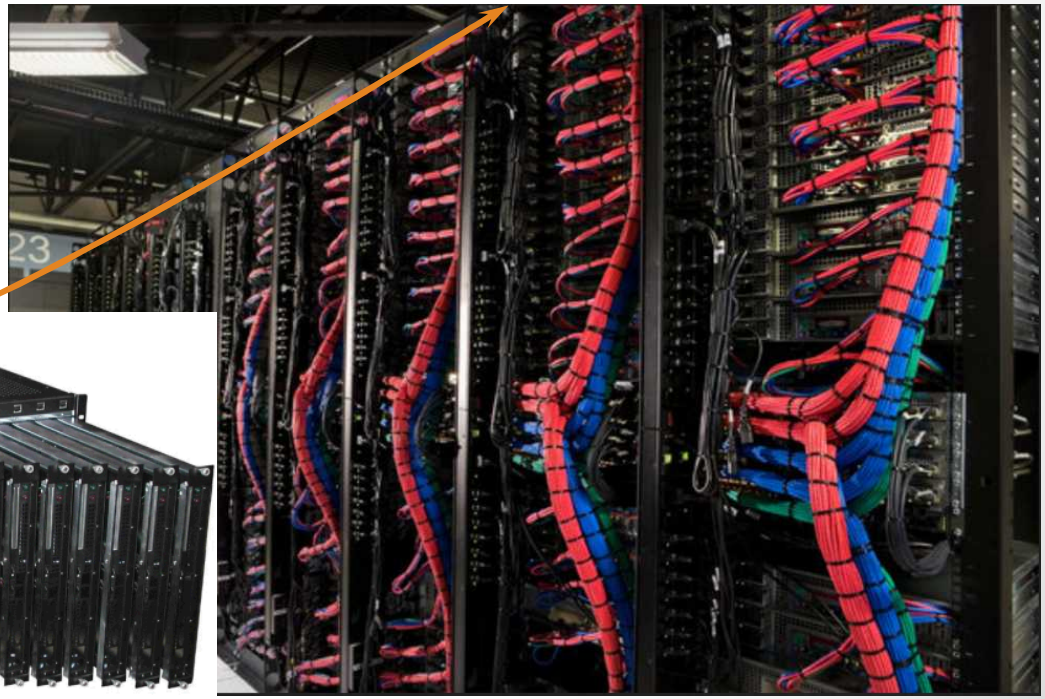

Server Rack

Blade Server

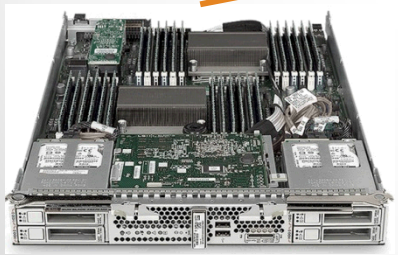

Silicon Photonics

SOItech SmartCut™ Process

1. Initial silicon
2. Thermal Oxidation
3. H+ implantation
4. Cleaning & bonding
5. Splitting
6. Annealing & CMP
   Touch polishing

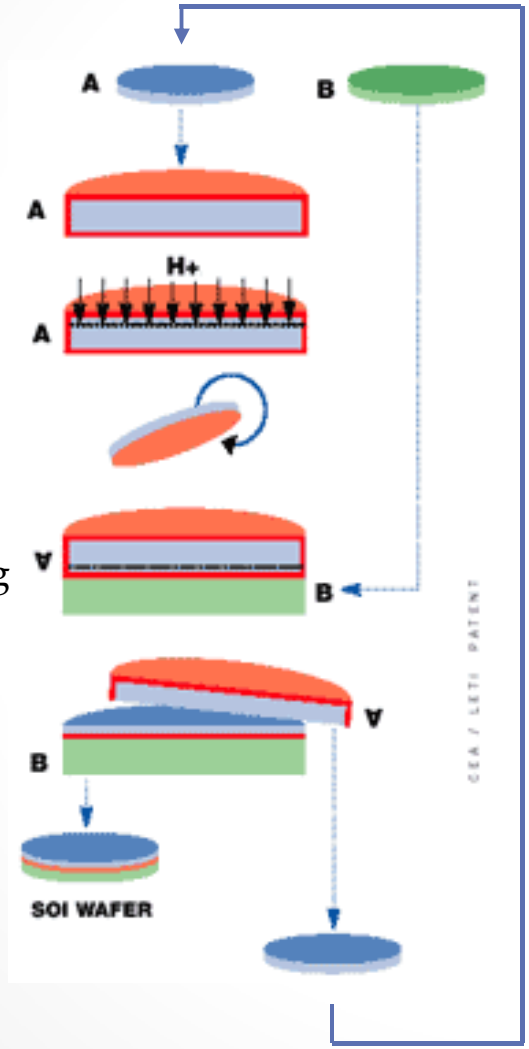

Why SOI?

- CMOS front-end compatible.
- High refractive index contrast ($\Delta n \sim 2.0$).
- Device layer can be doped
  - Monolithic integration of electronics/photonics.
- Low absorption loss at telecom wavelengths.

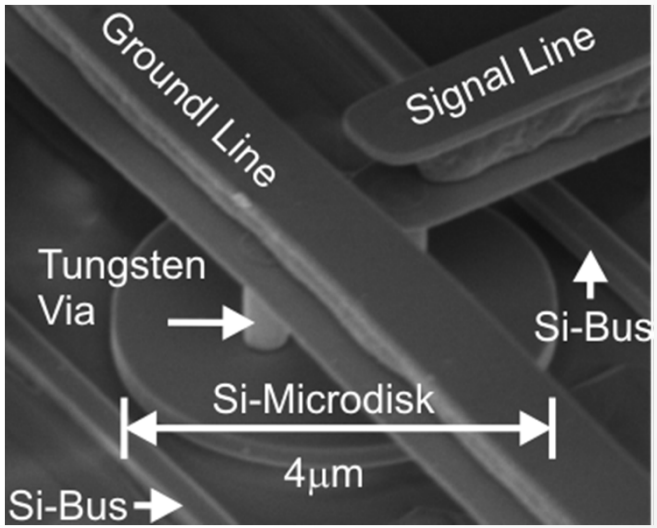

M.R. Watts, Opt. Express **19,** 21989-22003 (2011)

Outline

Scope of Thesis

- Investigation of waveguide crossings in multi-layer optical interconnection networks.
- Analysis a novel insertion loss measurement technique – the racetrack resonator loss platform.
- Statistical behavior of signals in rough waveguides and resonators due to Rayleigh scattering.

Defense Outline

Data Demands	Silicon Photonics	• Intro to waveguide crossings • Planar comparables • The NOS crossing • NOS optical modes • Crosstalk estimation • NOS crosstalk data • NOS loss data • Loss tradeoff analysis • Example design optimization • Conclusion	• Intro to loss measurement • Racetrack loss platform • Resonator transmission • Loss calibration • Width taper test case • Reference resonator data • Propagation loss data • Width taper data analysis • Example use cases • Conclusion	• Speckle in rough waveguides and resonators. • Intro to waveguide roughness • Random phasor sums • Quadratic EDF testing • Reflected intensity • Transmitted intensity • Estimating roughness size • Resonance splitting • Conclusion	Conclusion

Waveguide Crossings in OEICs

- Challenges in designing complex photonic interconnection networks
  - Each waveguide crossing causes attenuation and crosstalk.
  - Number of waveguide crossings scales with number of channels.
  - Number of crossings traversed varies by channel.
  - On-chip area scales with number of channels.
- No perfect planar solution exists.
- Multi-layer crossings suggested, but performance data not measured.

Here, we will explore the design space surrounding a CMOS compatible silicon nitride over SOI 3D optical layer for photonic interconnection networks and compare the results with single layer approaches.

- Review of competing planar technologies.
- Description of developed multi-layer solution.
- Presentation of crosstalk and loss data as a function of layer separation.
- Discussion of loss tradeoff between vertical transitions and waveguide crossing.
- Example optimization of a simplistic optical interconnect.

SOI Planar Waveguide Crossings

a)

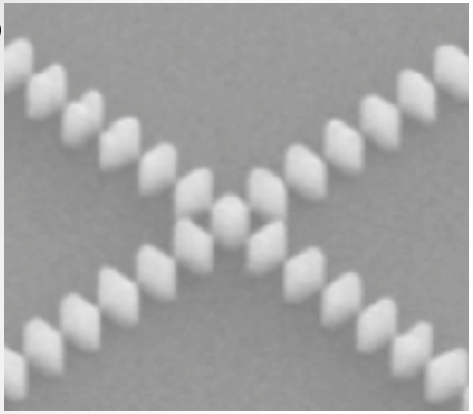

	< 0.1 dB Insertion Loss	< -40 dB Crosstalk	< 5 μm^2 On-chip Area	Broad Response (C-Band)	Fabrication Tolerant	Reference
Subwavelength Grating[a]	✓	✓				P. J. Bock, Opt. Exp. **18**, 16146-16155 (2010).
Photonic Crystal[b]	✓	✓				S. Lan, Opt. Lett. **27**, 1567-1569 (2002).
Anti-resonant	✓	✓	✓			S. G. Johnson, Opt. Lett. **23**, 1855-1857 (1998).
Wavefront Matching	✓					Y. Sakamaki, IEEE PTL 18, 2005-2007 (2006).
Multimode Interference			✓	✓	✓	H. Chen, IEEE PTL **18**, 2260-2262 (2006).
Mode Transformation[c]		✓	✓	✓	✓	W. Bogaerts, Opt. Lett. **32**, 2801-2803 (2007).

b)

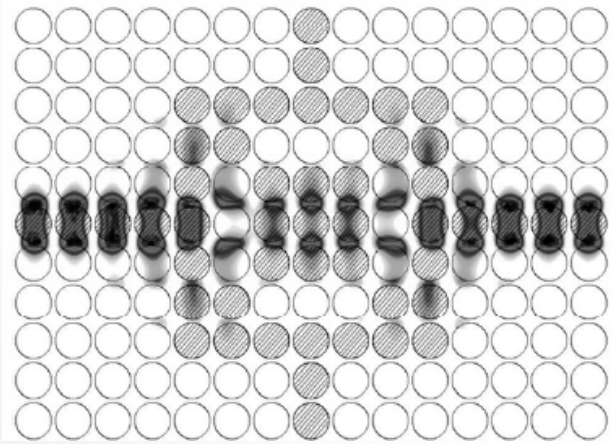

c)

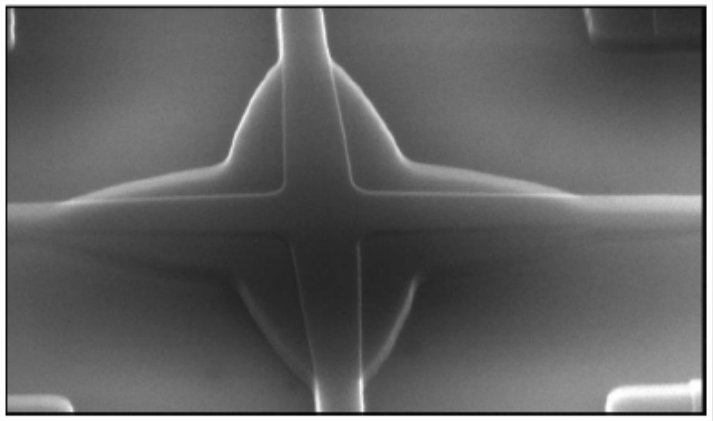

SiN over SOI (NOS) Waveguide Crossings

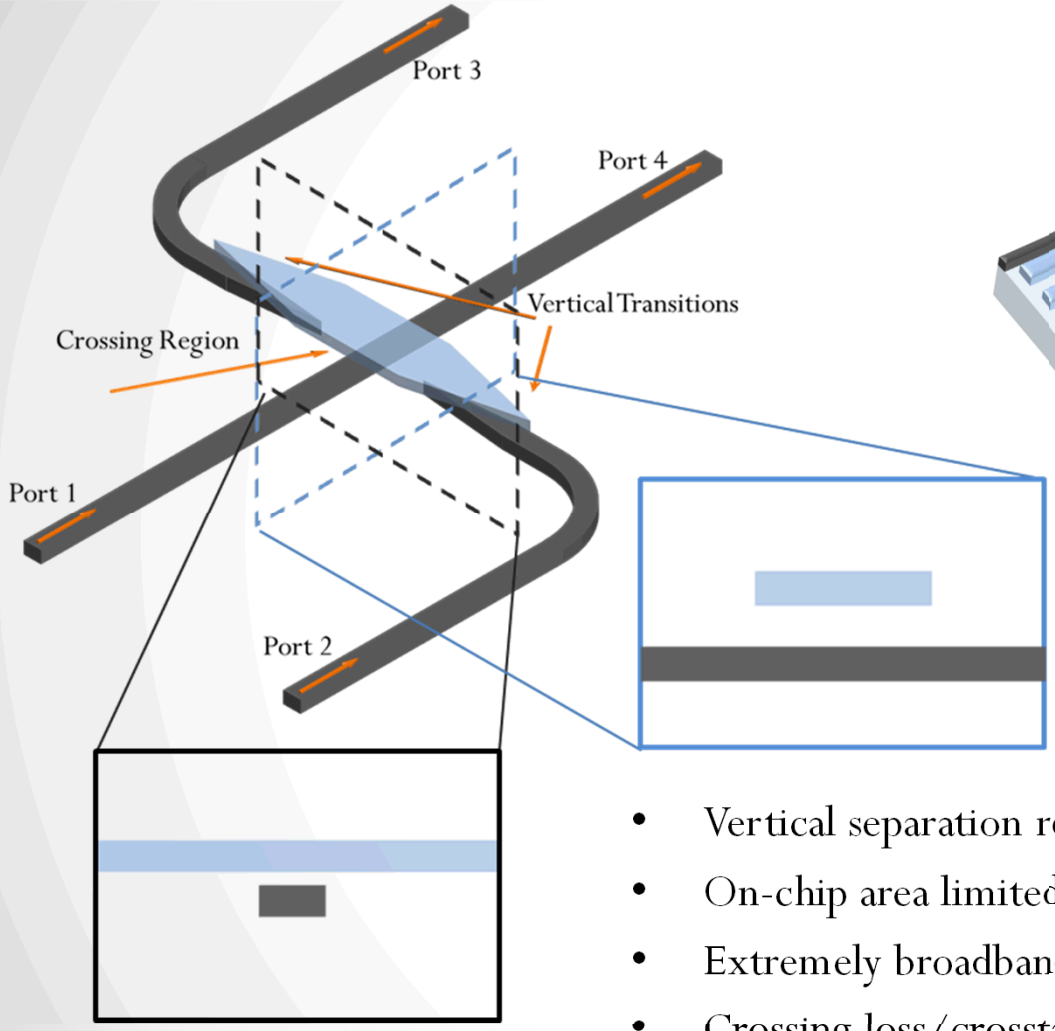

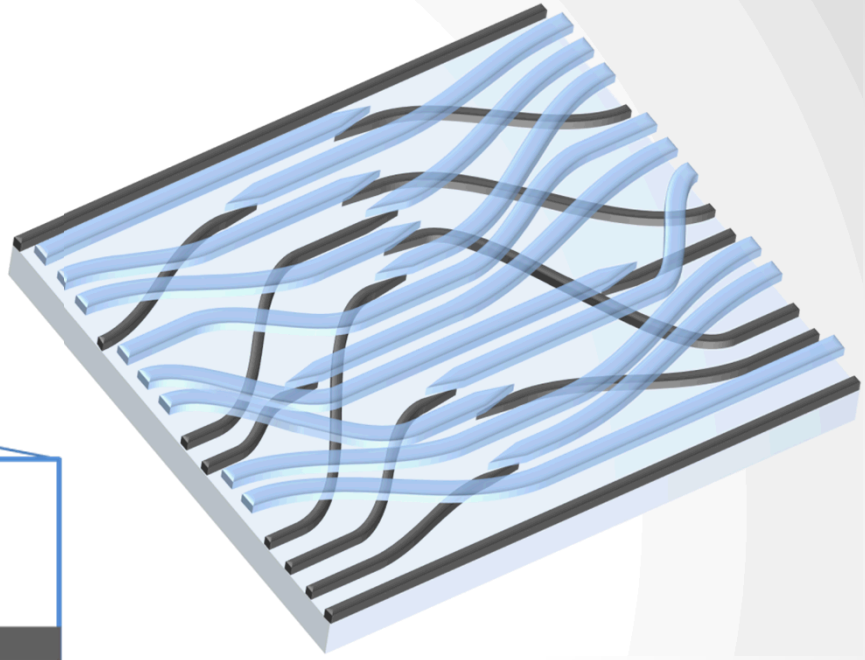

- Vertical separation reduces modal overlap with crossing guide.
- On-chip area limited to the product of the guide widths.
- Extremely broadband and fabrication tolerant.
- Crossing loss/crosstalk decrease as a function of layer separation.
- Vertical transition loss increases as a function of layer separation.

Crossing Mode – SOI, TE

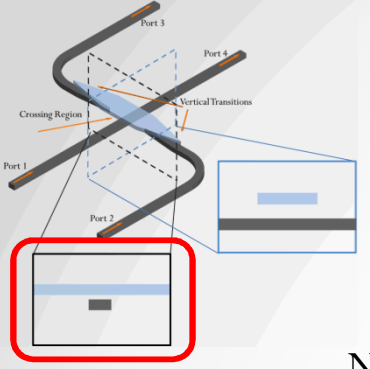

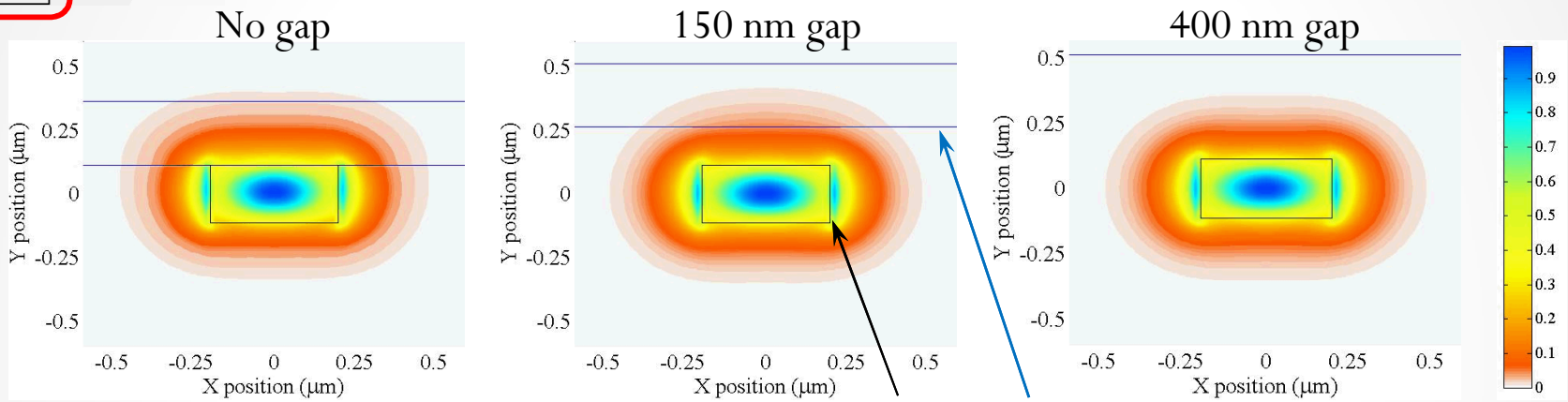

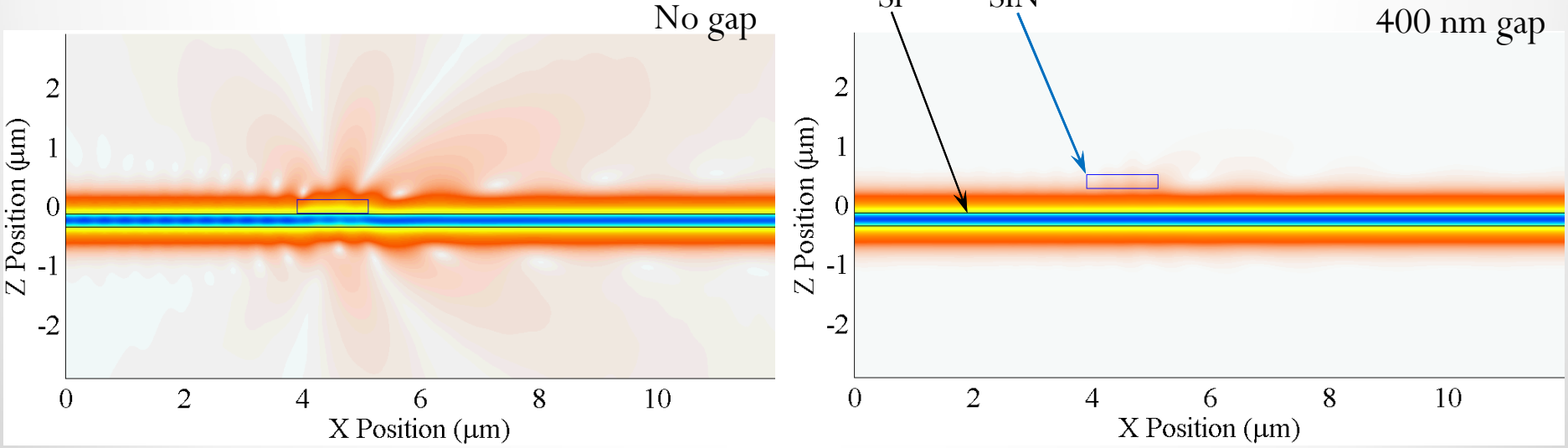

Crossing Mode – SiN, TE

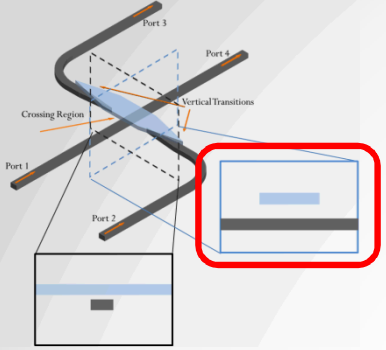

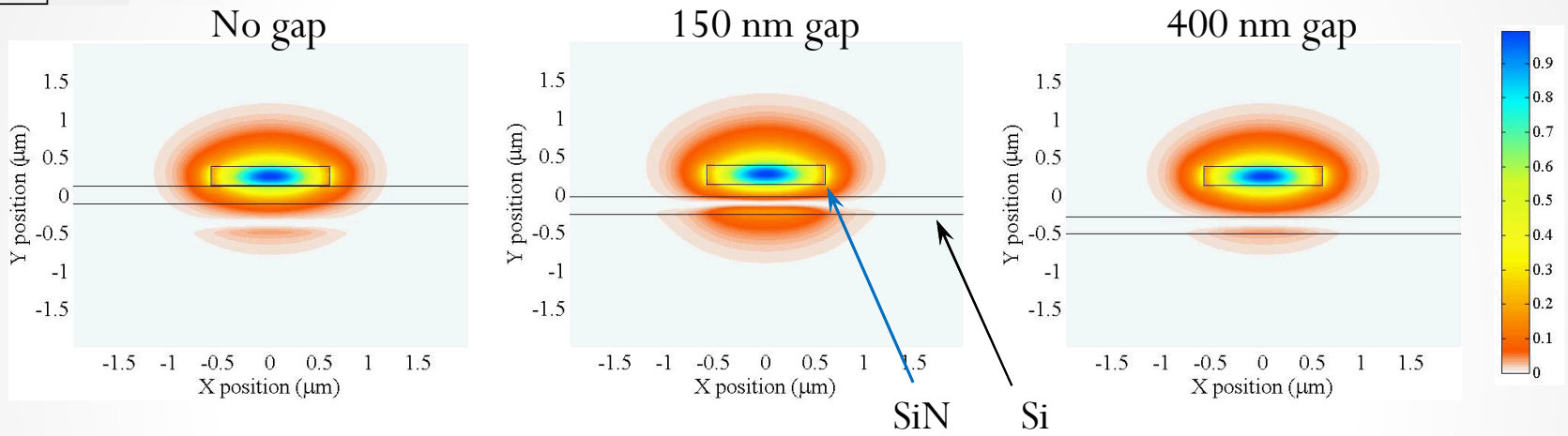

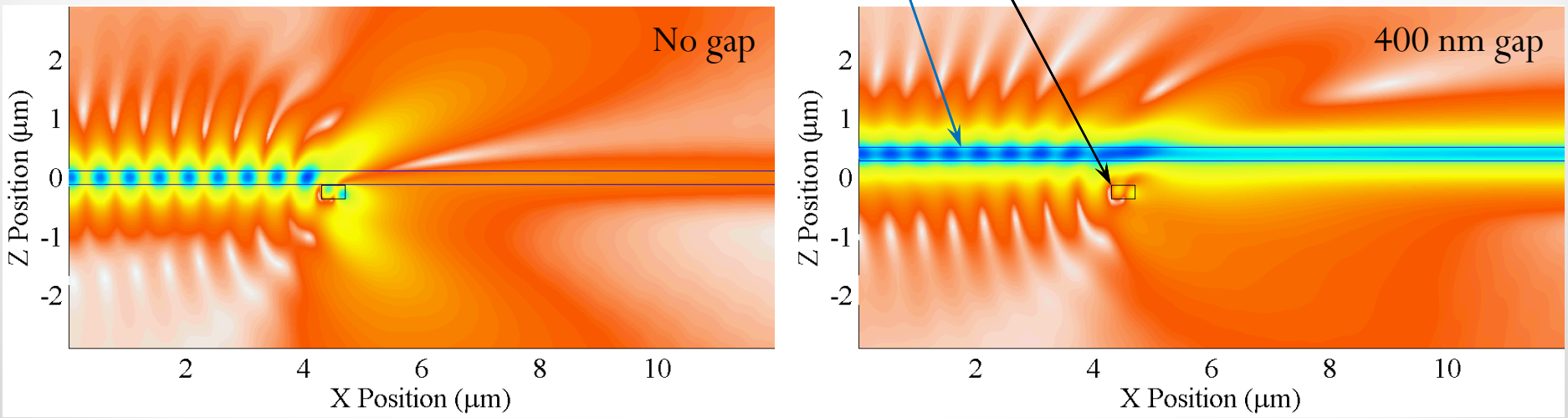

Measuring Crosstalk

Externally Measured (port-to-port) Crosstalk

$$EXT_1 \approx \frac{P_{13}}{P_{14}} = \frac{\eta_1\eta_3 L_1 L_3 \kappa_{13} P_0}{\eta_1\eta_4 L_1 L_4 \kappa_{14} P_0} = \frac{\eta_3 L_3 \kappa_{13}}{\eta_4 L_4 \kappa_{14}}$$

$$EXT_2 \approx \frac{P_{24}}{P_{23}} = \frac{\eta_2\eta_4 L_2 L_4 \kappa_{24} P_0}{\eta_2\eta_3 L_2 L_3 \kappa_{23} P_0} = \frac{\eta_4 L_4 \kappa_{24}}{\eta_3 L_3 \kappa_{23}}$$

Crosstalk Caused by the Crossing

$$XT_1 = \frac{\kappa_{13}}{\kappa_{13}+\kappa_{14}} \approx \frac{\kappa_{13}}{\kappa_{14}} \quad and \quad XT_2 = \frac{\kappa_{24}}{\kappa_{23}+\kappa_{24}} \approx \frac{\kappa_{24}}{\kappa_{23}}$$

Geometric Mean

$$EXT_1 \times EXT_2 \approx \frac{\eta_3 L_3 \kappa_{13}}{\eta_4 L_4 \kappa_{14}} \times \frac{\eta_4 L_4 \kappa_{24}}{\eta_3 L_3 \kappa_{23}} = \frac{\kappa_{13}}{\kappa_{14}} \frac{\kappa_{24}}{\kappa_{23}} \approx XT_1 \times XT_2$$

- The geometric mean of the externally measured crosstalk is an accurate approximation of the geometric mean of the device crosstalk.

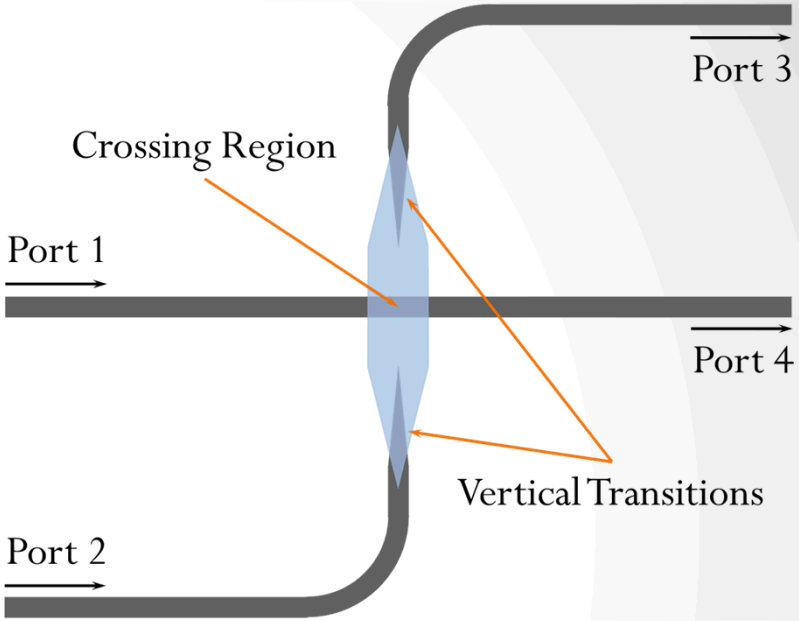

κ_{ij}	Power coupled from i to j by the crossing
EXT	Externally measured (port-to-port) crosstalk
XT	Crosstalk caused by the crossing
η_i	Fiber-to-waveguide coupling efficiency, port i
L_i	Path loss from port i to the crossing
P_0	Input power
P_{ij}	Power measured in port j for input port i

Crosstalk

TE Response

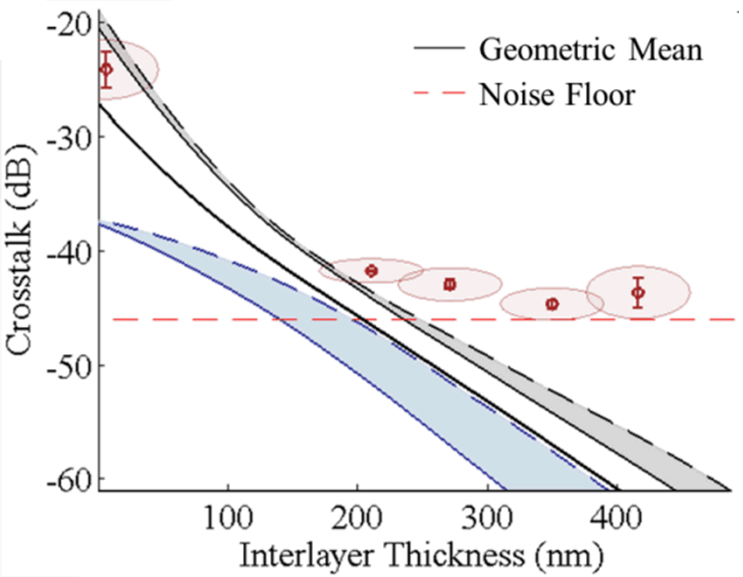

TM Response

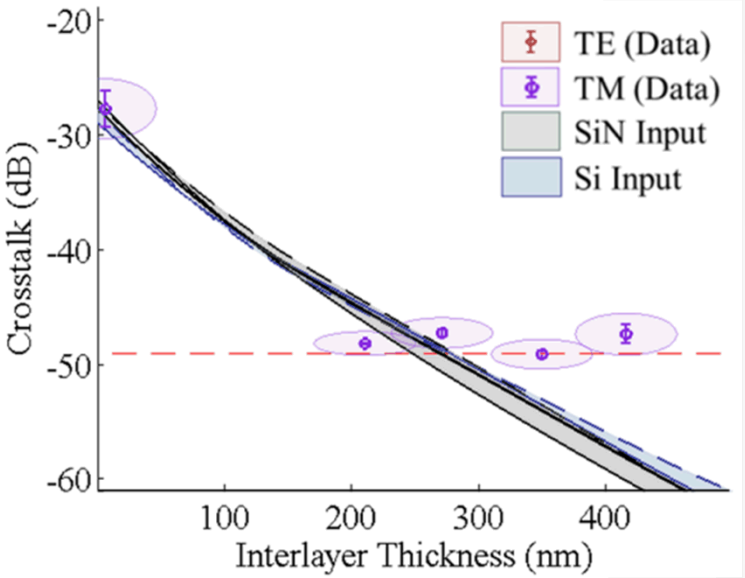

Experimental Setup

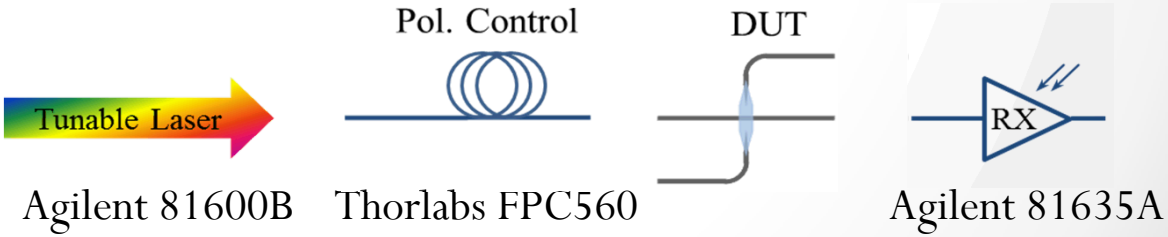

- Solid line → $\lambda = 1500$ nm
- Dashed line → $\lambda = 1600$ nm
- XT(λ) → ~ linear
- Scan step size → $\delta\lambda = 1$ pm

Excess Loss

Si Input

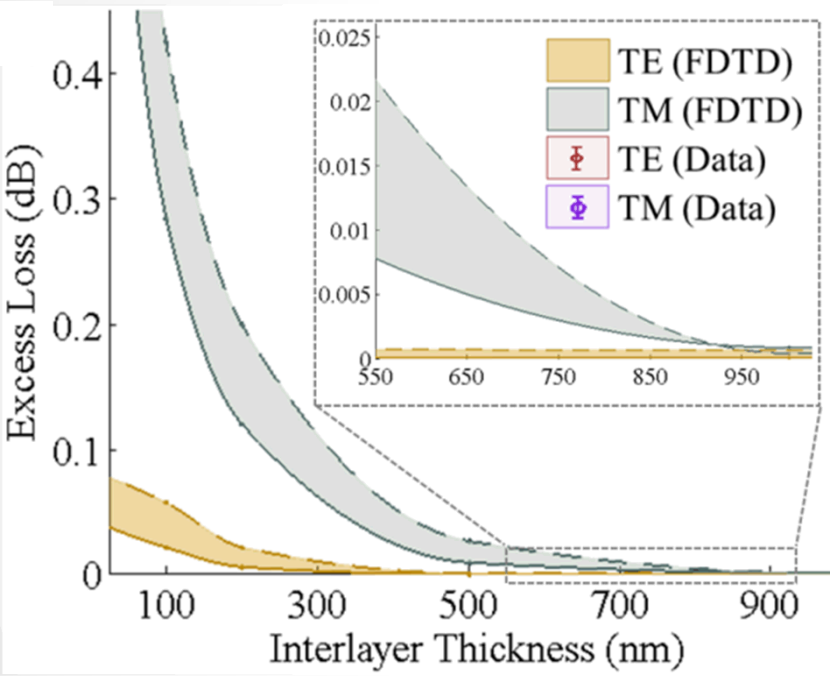

SiN Input

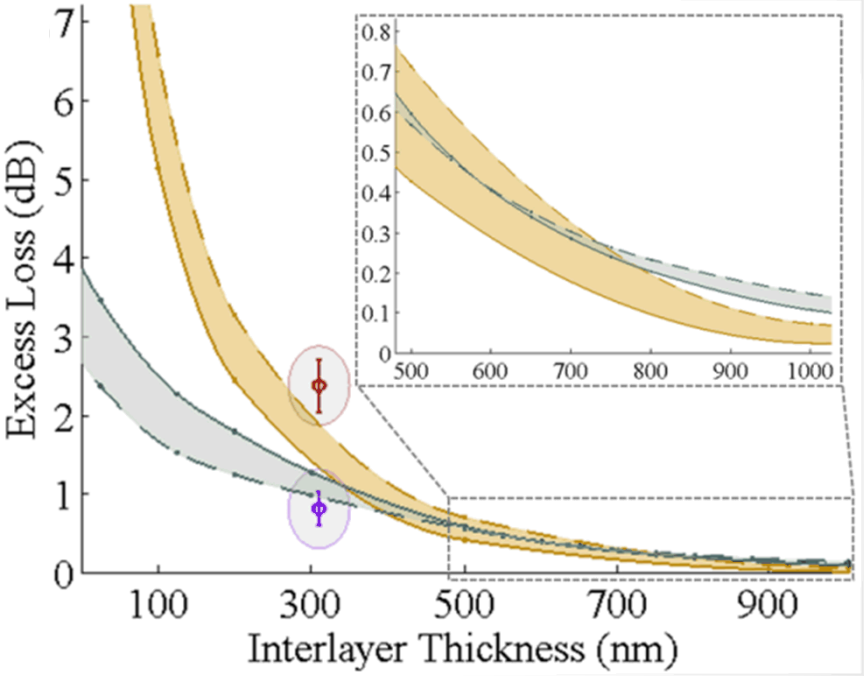

- Solid line → $\lambda = 1500$ nm
- Dashed line → $\lambda = 1600$ nm
- XT(λ) → ~ linear
- Scan step size → $\delta\lambda = 1$ pm

Loss Tradeoff

- Crossing dominates loss for small gaps.
- Transition dominates loss for large gaps.
- Break-even point depends on transition length and number of crossing per transition.

TE Response

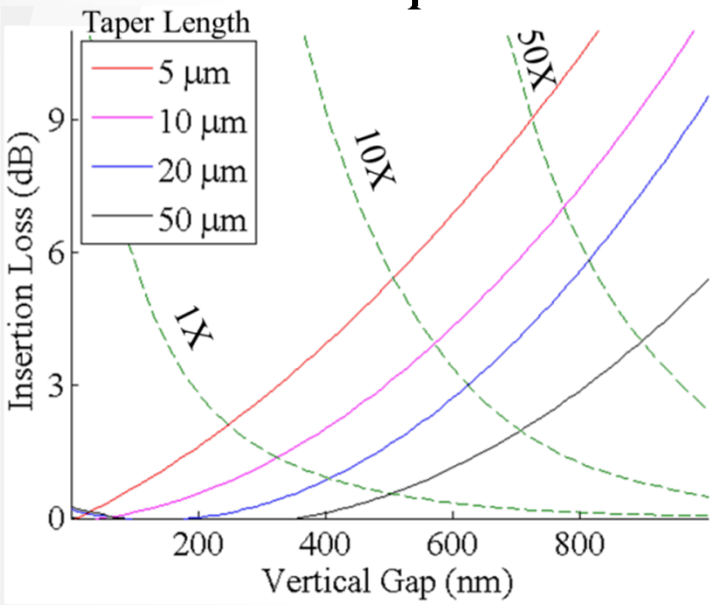

TM Response

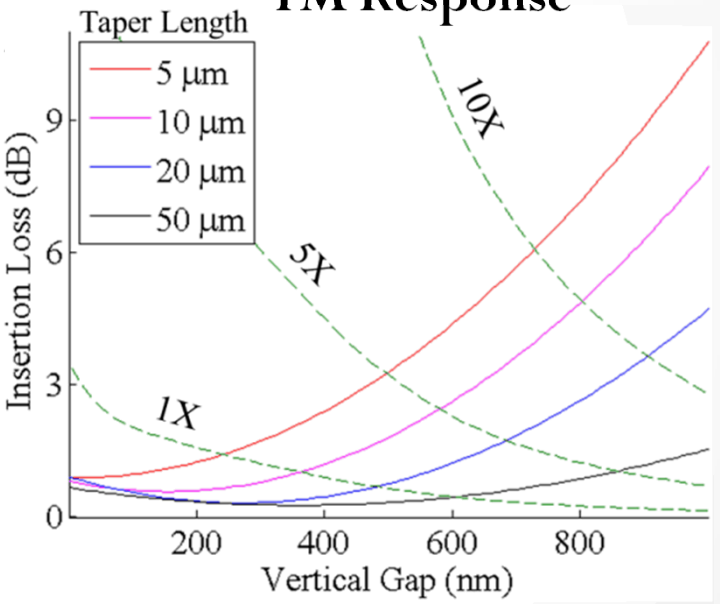

- Solid lines → transition loss
- Dashed lines → crossing loss
- $\lambda = 1550$ nm
- NX label → # crossings

Example Optimization

Example: Single waveguide with N crossings

- Compare to planar structure (W.Bogaerts, Opt. Lett. **32**, 2801-2803 (2007)).
- Determine optimal vertical gap.
- Determine optimal transition length.

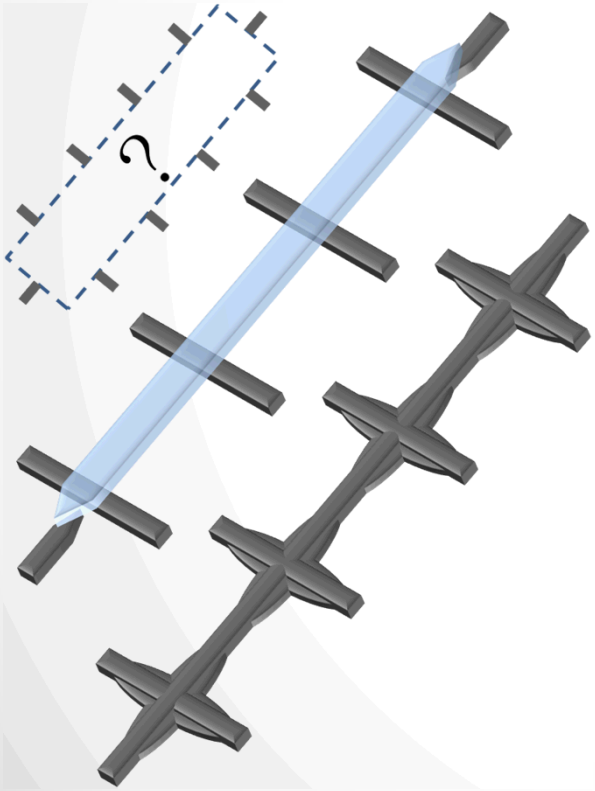

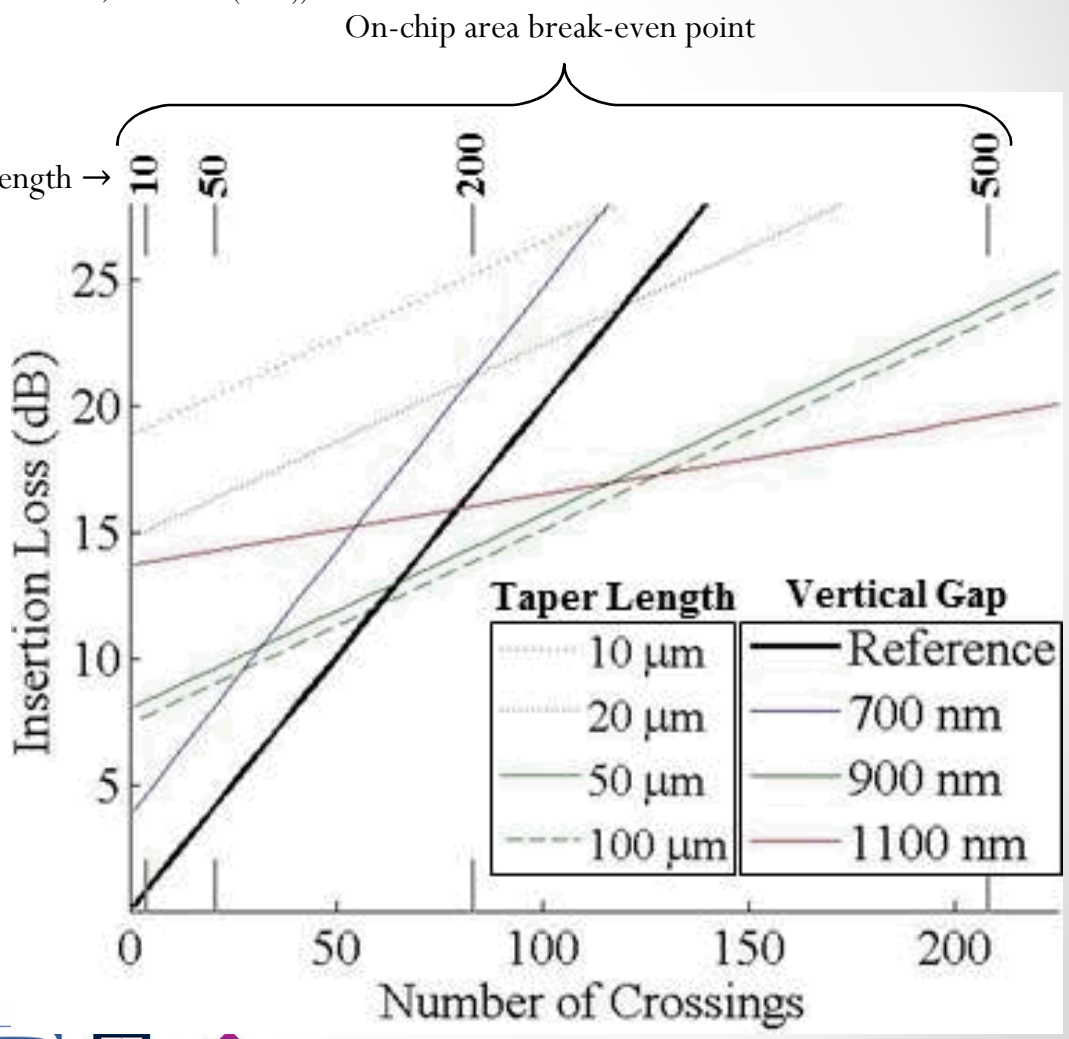

NOS Crossing

Conclusions

- Loss and crosstalk values for the SOI waveguide are exceptionally low.
- The SiN waveguide experiences over an order of magnitude larger insertion loss.
- The geometric mean of the externally measured crosstalk values is an accurate estimator of the geometric mean of the device crosstalk.
- Planar structures outperform the NOS crossings for optical paths with less than 75 crossings.
- NOS crossings require significantly lower on-chip area than efficient planar comparables.

Future Work

- Explore new materials for use as a secondary optical layer.
- Modify SiN guide geometry to enhance confinement.
- Modify crossing geometry to minimize modal interaction.

Racetrack Resonator Loss Platform (RLP)

- Start with a standard racetrack resonator configuration.
- Replace section 3 with a mirror-image version of the test structure.
- Transmission function fitting yields insertion loss of the test device.
- Appropriate calibration yields insertion loss of the test structure.

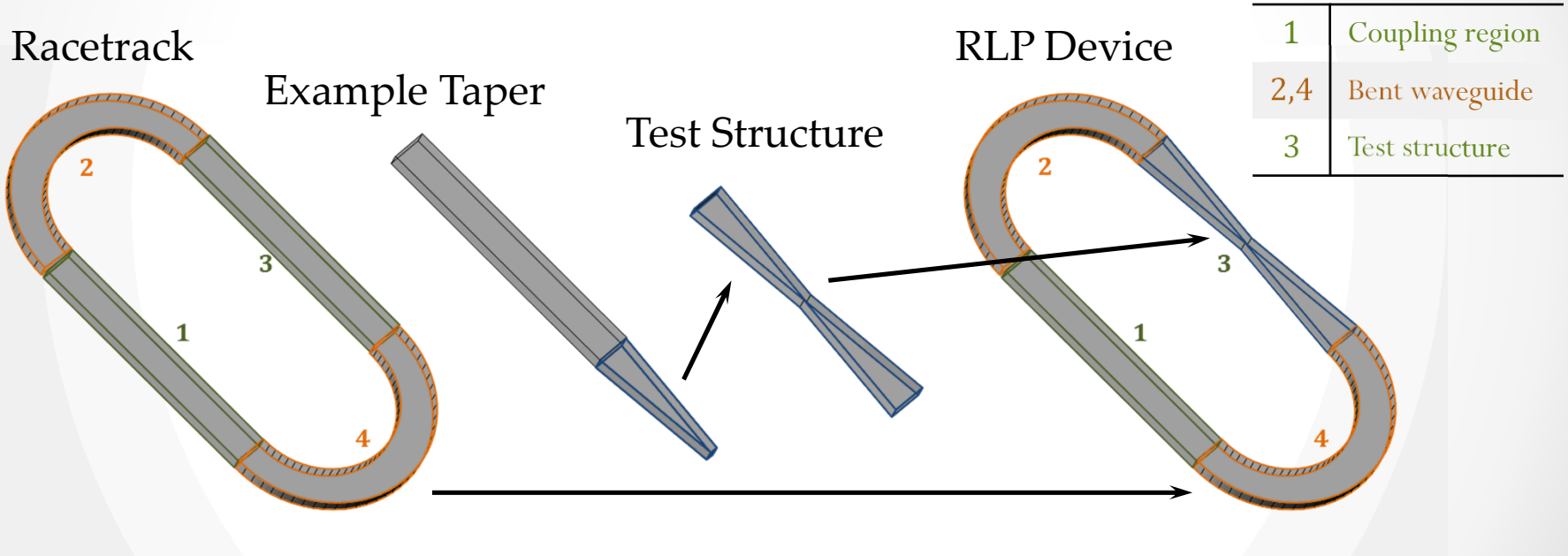

➢ Enables accurate insertion loss measurement for compact, efficient photonic devices.

- Review -> Theory -> Calibration -> Experimental Results for lateral tapers

Loss Measurement Overview

	Pros	Cons
Cut-back 	• Easily implemented. • Suitable for insertion and propagation Loss.	• Alignment error and fabrication variations affect loss estimate. • Requires a large number of devices.
Liquid Prism 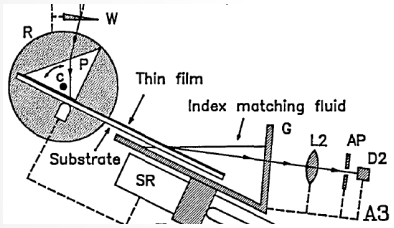	• Single device required. • Suitable for insertion and propagation loss.	• Requires a liquid with higher refractive index than the waveguide.
Ring Resonator 	• Single device required. • Capable of measuring very low loss (< 1dB/m).	• Susceptible to bend loss. • Difficult to measure insertion loss.

Resonator Transfer Function

- Contra-directional coupling with rate γ_β causes doublet formation.
- Response of doublet given by coherent addition of two singlets corresponding to standing wave modes with sinusoidal and cosinusoidal azimuthal dependence.

$$E^{c,s} = \frac{\kappa}{i\left(\Delta\omega \pm \gamma_\beta/2\right) - \gamma_\alpha^{c,s}/2} \qquad T = \left| -1 + \frac{\kappa}{\sqrt{2}}\left(E^c + E^s\right)\right|^2$$

- Loss rate and loss coefficients are related by the Q-factor.

$$Q_\alpha = \frac{\omega_0}{\gamma_\alpha} = \frac{2\pi n_g L}{\lambda_0 \ln(\alpha)}$$

- Assuming doublet converges to singlet as $\gamma_\beta \to 0$, the device loss rate can be calculated.

$$\gamma_\alpha = \overline{\gamma_\alpha^{cs}}\left(1 + \left(\delta_\alpha^{cs}/\overline{\gamma_\alpha^{cs}}\right)^2\right) \quad with \quad \begin{cases} \overline{\gamma_\alpha^{cs}} = (\gamma_\alpha^c + \gamma_\alpha^s)/2 \\ \delta_\alpha^{cs} = (\gamma_\alpha^c - \gamma_\alpha^s)/2 \end{cases}$$

- Insertion loss is then determined from the loss coefficient via $IL = 10\log_{10}(\alpha^2)$.

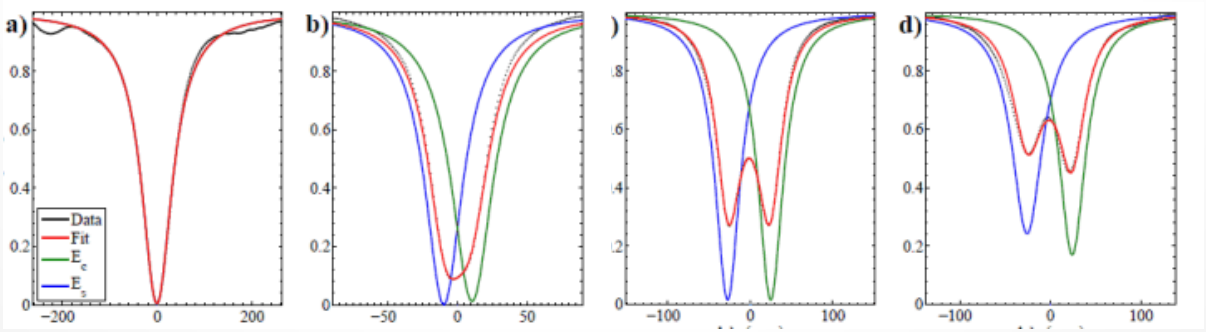

RLP – Loss Measurement Calibration

$$IL_{DUT} - IL_{REF} + IL_3 = IL_{SUT} = 2 \cdot IL_{TAPER}$$

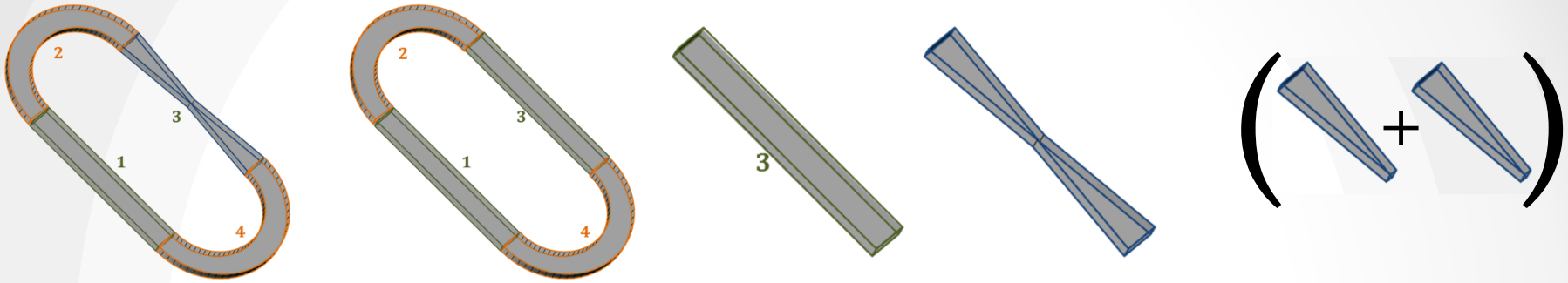

$$IL_{DUT} = IL_{SUT} + \sum_{i=1,2,4} IL_i + 4 \cdot IL_{STB} \qquad IL_{REF} = \sum_{i=1}^{4} IL_i + 4 \cdot IL_{STB}$$

Cal. #	$\widehat{IL}_{SUT}$	$err(\widehat{IL}_{SUT}) = IL_{SUT} - \widehat{IL}_{SUT}$
0	IL_{DUT}	$err(\widehat{IL}_{DUT}) + \sum_{i=1}^{3} IL_i + 4 \cdot IL_{STB}$
1	$IL_{DUT} - IL_{REF}$	$err(\widehat{IL}_{DUT}) - IL_3 + err(\widehat{IL}_{REF})$
2	$IL_{DUT} - IL_{REF} + IL_3$	$err(\widehat{IL}_{DUT}) + err(\widehat{IL}_3) + err(\widehat{IL}_{REF})$

- We will see that $IL_3 \ll IL_{REF}$ in the example devices presented here.

RLP Test Case – Core Width Taper

- Test unit comprised of symmetric, mirror-image tapers.
- Taper from 400nm initial to 250nm final waveguide width
- Linear, Parabolic, Exponential, and linear n_{eff} taper functions.
- 2.5, 5, and 10\um long tapers.
- Bus width.
- Lateral separation.
- Reference resonators.

Function	w(x)	Taper	SUT
Exponential	$250 + 150e^{-5(1-\|x\|/L)}$	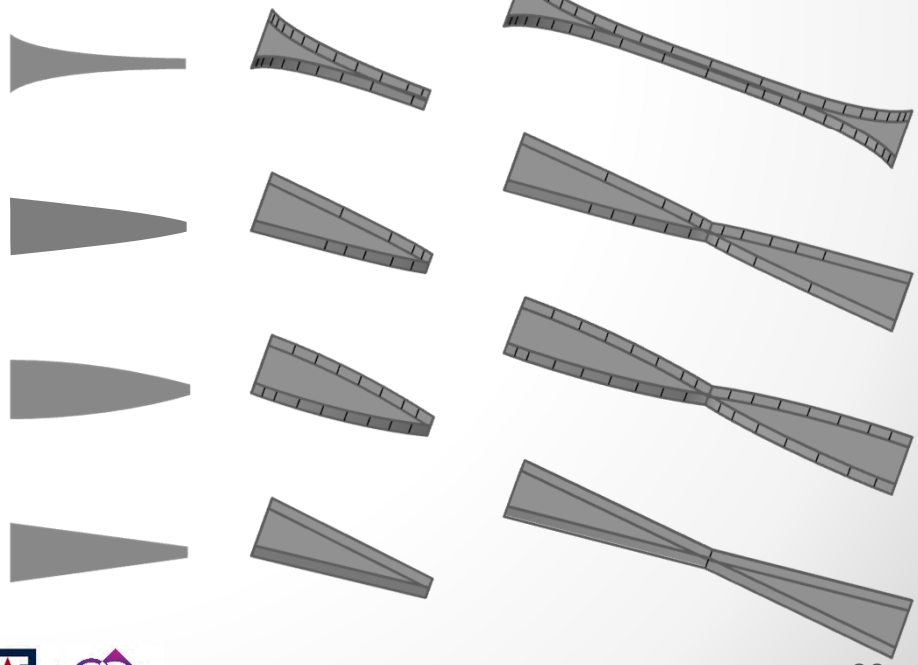	
Linear n_{eff}			
Parabolic	$250 + 150(\|x\|/L)^2$		
Linear	$250 + 150 \cdot \|x\|/L$		

Calibration - Reference Resonators

- Standard structure, no SUT.
- Confidence interval of 0.0063dB.
- Add resonator geometry

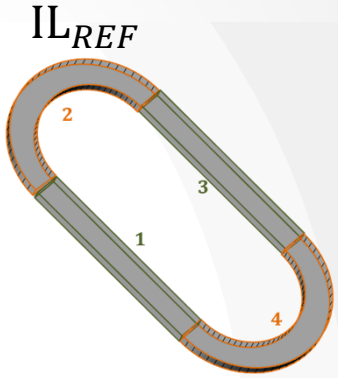

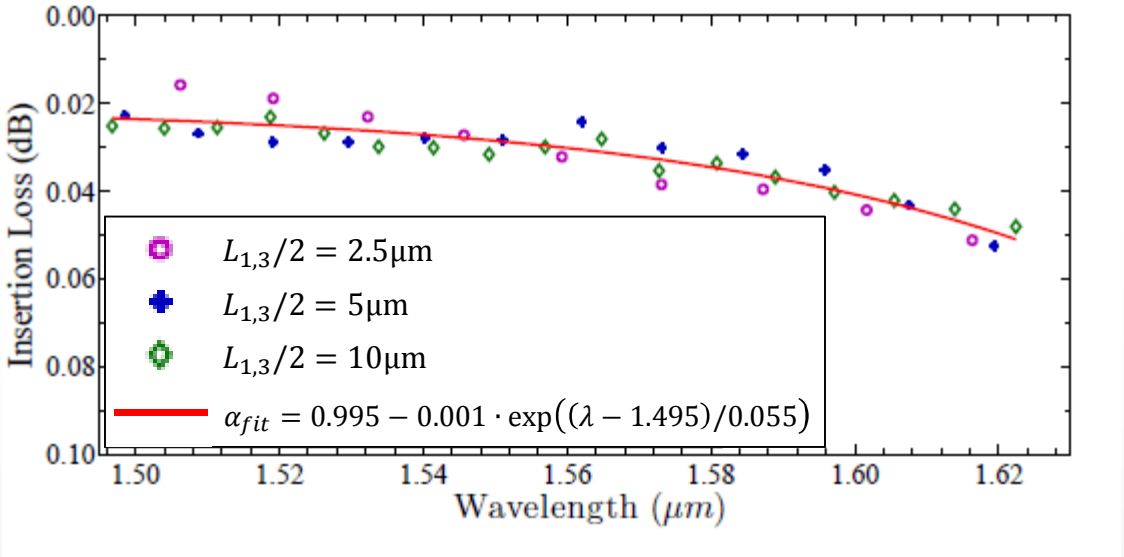

Propagation Loss Estimation - Cutback

- S-bend structures used to vary total length of straight waveguide sections only.
- Propagation loss estimated by slope of linear fit to insertion loss as a function of straight length.

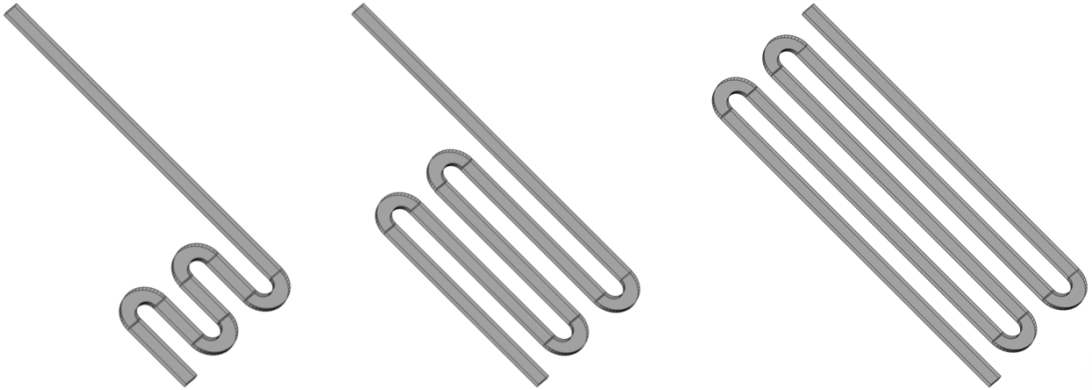

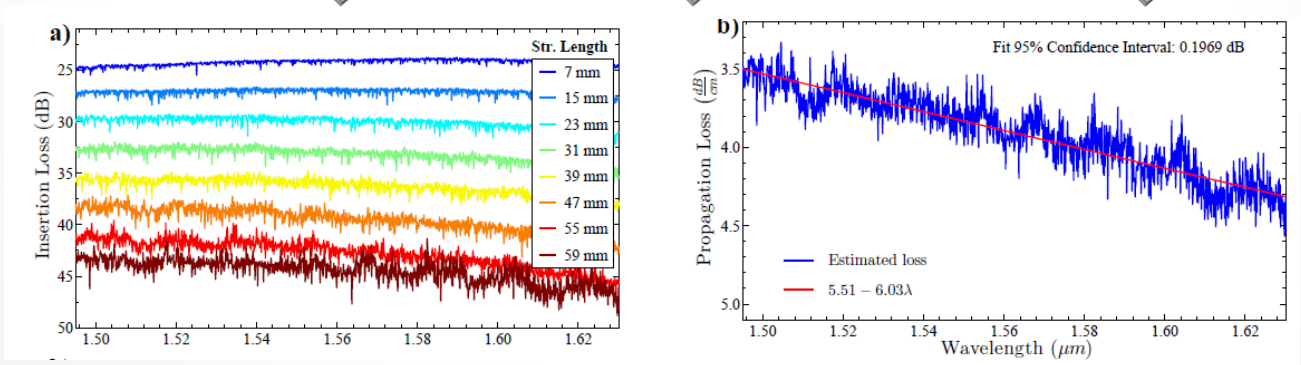

Insertion Loss Data

- IL_{DUT} (data)
- IL_{DUT} (fit)
- $IL_{DUT} - IL_{REF}$ (fit)
- $IL_{DUT} - IL_{REF} + IL_3$ (fit)

❖ Y-scale changes for each taper length.

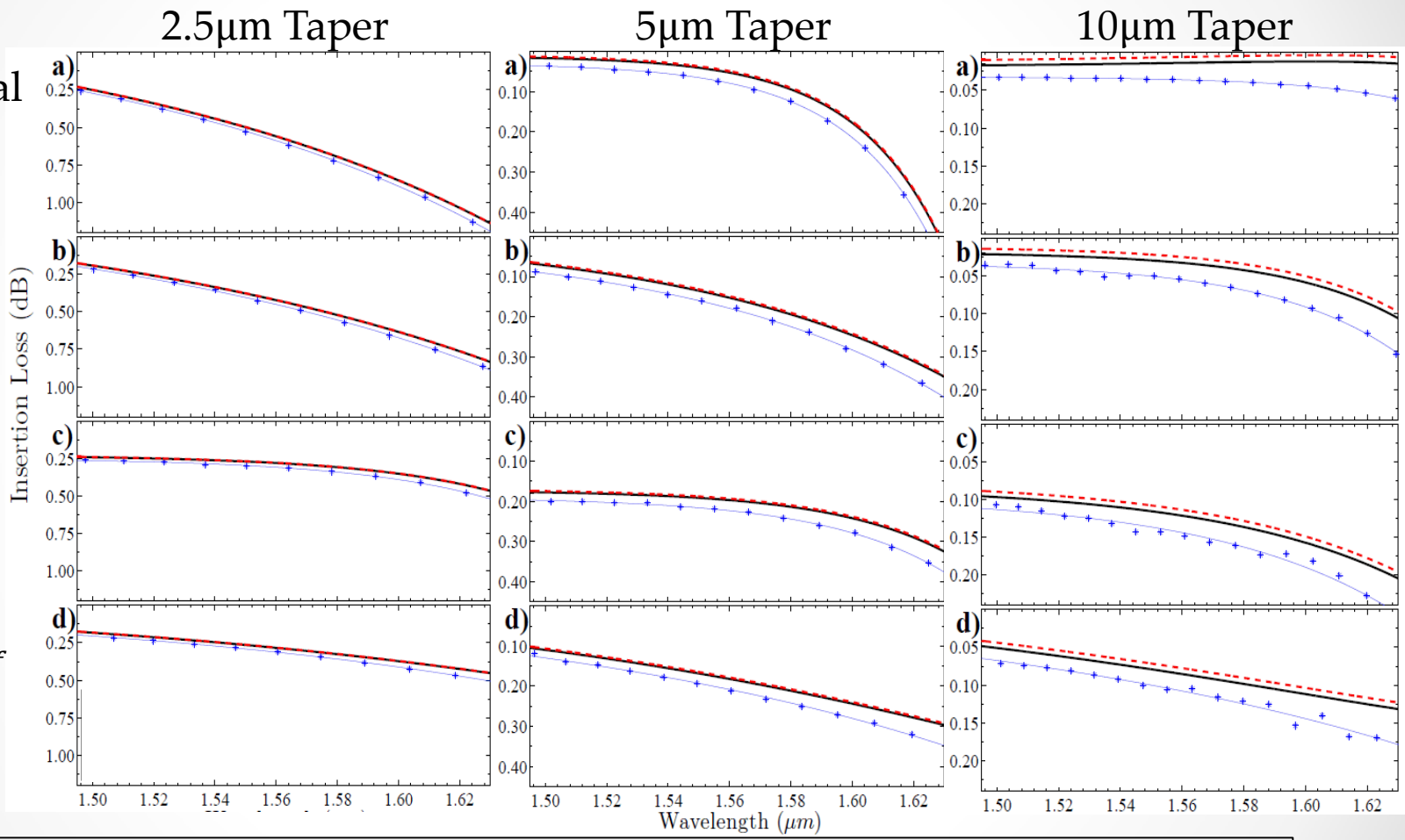

- Statements about which tapers perform in which regimes, trends, etc.
- Estimated error values.
- Change Legend entries to IL values

Other Examples

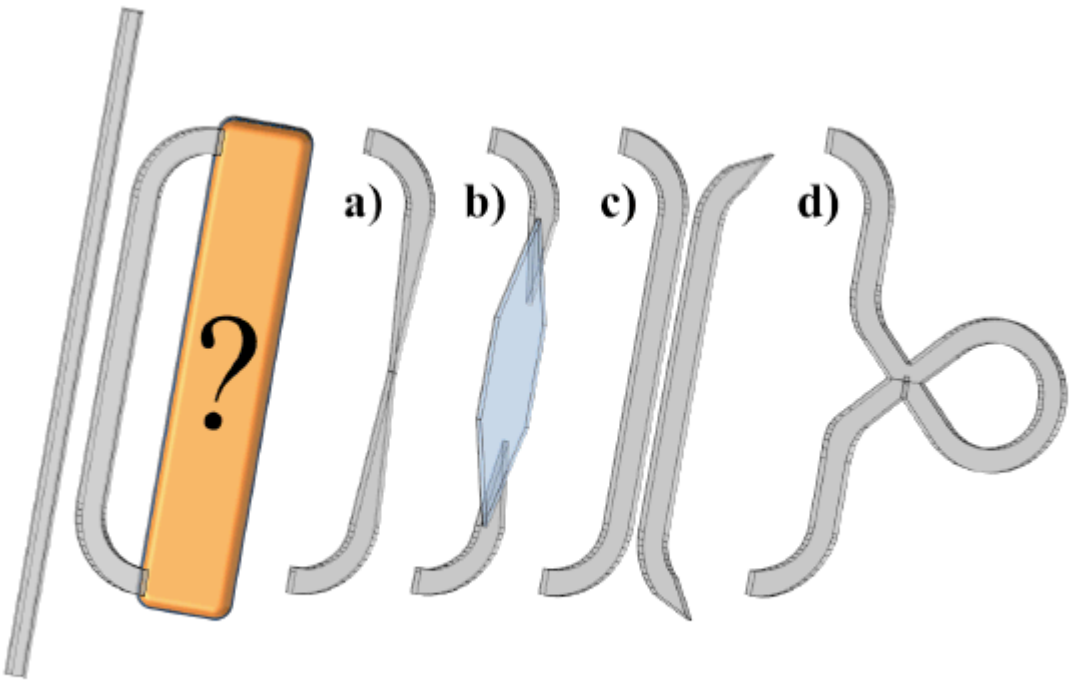

Figure 3.1: Racetrack resonator with example test structures: a) lateral taper, b) vertical transition, c) tap coupler, and d) waveguide crossing.

Racetrack Resonator Loss Platform

Conclusions

- The RLP enables accurate analysis of the insertion loss of efficient, compact structures.
- The RLP is suitable for a variety of structures including waveguide tapers, vertical transitions, optical tap couplers, and waveguide crossings to name a few.
- In the presented SOI example, a confidence interval of 0.0063dB was obtained.
- Calibration by a reference resonator will likely be suitable in most cases.
- Secondary calibration by an estimate of IL_3 provides exceptional accuracy.

Future Work

- Implement in additional material systems.
- Apply technique to various test cases.
- Explore upper and lower loss measurement limits.
- Attempt to improve measurement error.

Speckle in Rough Waveguides & Resonators

- Small roughness implies local mode is approximately that of the unperturbed waveguide.
- Scattering occurs when this mode impinges on a dielectric perturbation causing.

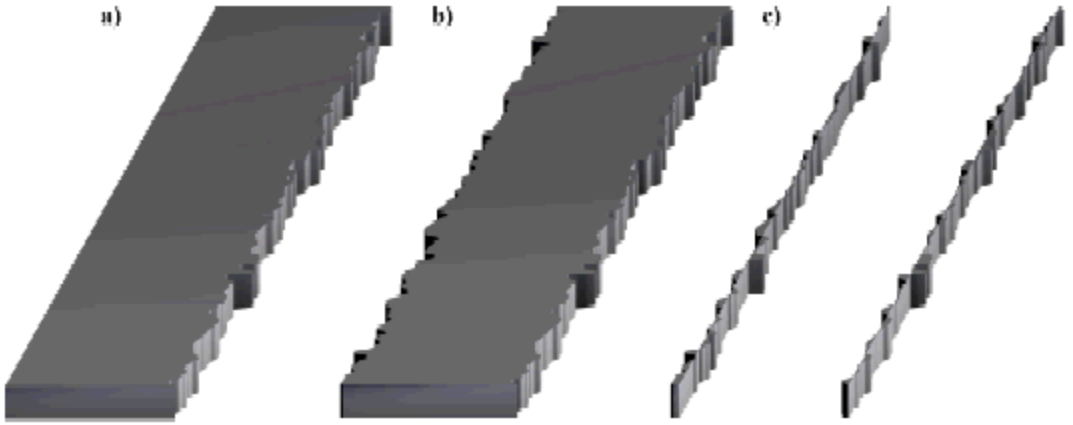

Figure 4.1: 3D representation of waveguides with (a)one and (b)two FISUR corrupted sidewalls along with (c)the sidewall roughness as a perturbation of the perfect waveguide.

$$K_{\mu\nu}(z) \approx f(z)\hat{K}_{\mu\nu}$$

$f(z) \rightarrow$ *deviation from ideal waveguide boundary*

$$\hat{K}_{\mu\nu} = \frac{i\omega\epsilon_0\delta\epsilon}{4P}\int_{-d}^{d} dy \left[E^*_{\mu t}\cdot E_{\nu t} + \gamma_K\left(H^*_{\mu x}\frac{\partial E_{\nu z}}{\partial y} + \frac{\partial H^*_{\mu y}}{\partial x}E_{\mu z}\right)\right]$$

$$\gamma_K = \begin{cases} 1/\left(\omega\epsilon_0 n_g\right)^2, & f(z) > 0 \\ 0, & f(z) = 0 \\ -1/\left(\omega\epsilon_0\right)^2, & f(z) < 0 \end{cases}$$

Scattering in Rough Waveguides

- Small roughness implies local mode is approximately that of the unperturbed waveguide.
- Scattering occurs when this mode impinges on a dielectric perturbation causing.

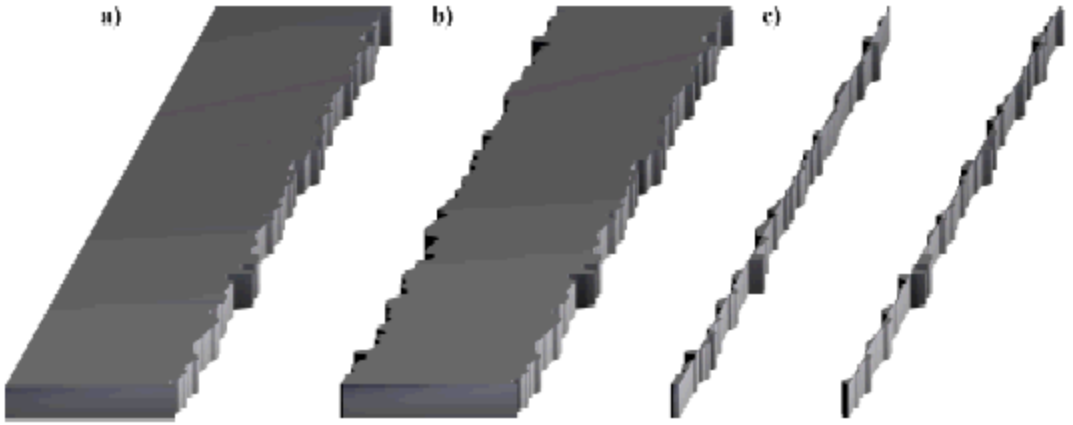

Figure 4.1: 3D representation of waveguides with (a)one and (b)two FISUR corrupted sidewalls along with (c)the sidewall roughness as a perturbation of the perfect waveguide.

$$K_{\mu\nu}(z) \approx f(z)\hat{K}_{\mu\nu}$$

$f(z) \rightarrow$ *deviation from ideal waveguide boundary*

$$\hat{K}_{\mu\nu} = \frac{i\omega\epsilon_0\delta\epsilon}{4P}\int_{-d}^{d} dy \left[E^*_{\mu t}\cdot E_{\nu t} + \gamma_K\left(H^*_{\mu x}\frac{\partial E_{\nu z}}{\partial y} + \frac{\partial H^*_{\mu y}}{\partial x}E_{\mu z}\right)\right]$$

$$\gamma_K = \begin{cases} 1/\left(\omega\epsilon_0 n_g\right)^2, & f(z) > 0 \\ 0, & f(z) = 0 \\ -1/\left(\omega\epsilon_0\right)^2, & f(z) < 0 \end{cases}$$

Random Phasor Sum

- Following Goodman[REF] and Dainty[REF], the distributions on the amplitude (A), intensity (I), and measured intensity (I') may be derived.
  1. Assumes a large number of statistically independent fields ($\boldsymbol{a}_k = |a_k|\exp(i\phi_k)$).
  2. Assumes the joint distribution on the real (r)and imaginary(i) components is Normal.
- Condition(1) satisfied by sufficient propagation length.
- Morichetti, et.al. [REF] demonstrated that rough waveguides obey (2) regardless of geometry, polarization, etc.

$$\boldsymbol{a} = \frac{1}{\sqrt{N}}\sum_{k=1}^{N}|a_k|e^{i\phi_k} \qquad p_{RI}(r,i) = \frac{1}{2\pi\sigma_{RI}^2}exp\left[\frac{-(r^2+i^2)}{2\sigma_{RI}^2}\right]$$

$$p(|A|) = \frac{2|A|}{\langle I\rangle}exp\left(\frac{-|A|^2}{\langle I\rangle}\right), \quad |A| \geq 0$$

$$p(I) = \frac{1}{\langle I\rangle}exp\left(\frac{-I}{\langle I\rangle}\right), \quad I \geq 0$$

$$p(I') = \left(\frac{n_0}{\langle I\rangle}\right)^{n_0}\frac{I'^{(n_0-1)}exp\left(-I'n_0/\langle I\rangle\right)}{\Gamma(n_0)}, \quad I' \geq 0$$

Quadratic EDF Testing

- Effectively OLS applied to the EDF.
- Zero mean, Normally distributed residuals a strong indicator of appropriate fit function.
  - Lack of bias indicates appropriate distribution shape found.
- Some distributions we will need are presented as well.

Statistical Behavior – Reflected Intensity

- Reflected intensity is simply a random phasor sum.
- Image from Morichetti, distribution, PDF & CDF plots.

Statistical Behavior – Transmitted Intensity (T)

- Conservation of energy yields transmitted intensity.
  - Distribution on forward scattered fields converges to Normal.
  - Lumping loss and reflected fields together ($S' = \alpha' - R'$) and performing a probability transformation give $p(S')$.

$$p(S') = \left(\frac{n_r}{\langle R \rangle}\right)^{n_r} \frac{(\bar{\alpha} - S')^{(n_r-1)} exp\left(-(\bar{\alpha} - S')' n_r / \langle R \rangle\right)}{\Gamma(n_r)}, \quad S' \leq \alpha'$$

- Inclusion of additive white noise (N') produces the final relation on T'.

$$p(T') = p(S') * p(\delta'_\alpha) * p(N')$$

- PDF with fit, CDF with fit, correlation function

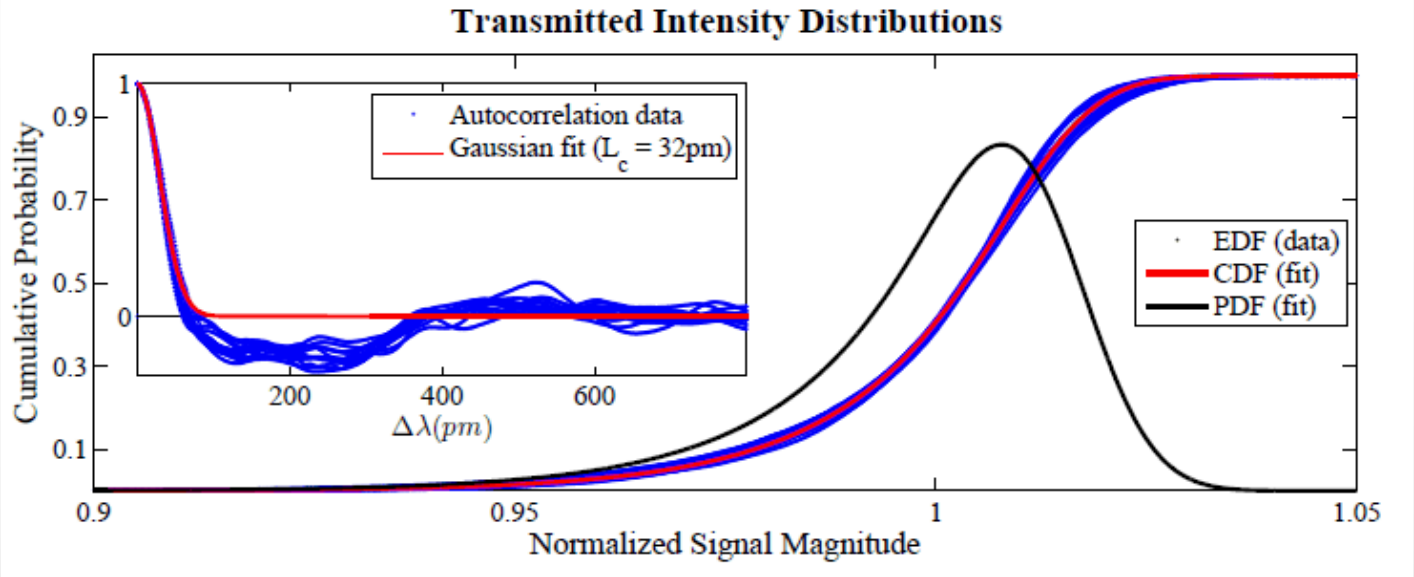

Estimating Roughness Size from T'

- Assume fit to transmission data noise provides an estimate of $\langle R \rangle$ and n_r.
- Link between $\langle R \rangle$ and $f(z)$ then obtained by the following equations

$$|a_k| = |f(z_k)|\hat{K}_{+-}(z_k) \qquad \text{and} \qquad \langle R \rangle = \langle |a_k|^2 \rangle = 2\sigma_{RI}^2$$

- Expressions can then be derived for $p(|a_k|)$

Low Permittivity Contrast, one rough boundary	Low Permittivity Contrast, two rough boundaries
$\lvert a_k\rvert_{l,1} = \lvert \kappa f_1(z_k)\rvert$	$\lvert a_k\rvert_{l,2} = \lvert \kappa f_1(z_k)\rvert + \lvert \kappa f_2(z_k)\rvert$
$p\left(\lvert a_k\rvert_{l,1}\right) = \mathrm{HN}(0, \kappa\sigma_{SW})$	$p\left(\lvert a_k\rvert_{l,2}\right) = \mathrm{HN}(0, \kappa\sigma_{SW}) * \mathrm{HN}(0, \kappa\sigma_{SW})$
High Permittivity Contrast, one rough boundary	**High Permittivity Contrast, two rough boundaries**
$\lvert a_k\rvert_{h,1} = \lvert \mathrm{C}_{1+}\rvert + \lvert \mathrm{C}_{1-}\rvert$	$\lvert a_k\rvert_{h,2} = \lvert \mathrm{C}_{1+}\rvert + \lvert \mathrm{C}_{1-}\rvert + \lvert \mathrm{C}_{2+}\rvert + \lvert \mathrm{C}_{2-}\rvert$
$p\left(\lvert a_k\rvert_{h,1}\right) = \mathrm{HN}(0, s_+) * \mathrm{HN}(0, s_-)$	$p\left(\lvert a_k\rvert_{h,2}\right) = \left(\mathrm{HN}(0, s_+) * \mathrm{HN}(0, s_-)\right) * \left(\mathrm{HN}(0, s_+) * \mathrm{HN}(0, s_-)\right)$

Variable Definitions

$$\mathrm{C}_{n+} = \kappa_+ f_n(z_k)\mathrm{U}(f(z_k)) \qquad \mathrm{C}_{n-} = \kappa_- f_n(z_k)\left(1 - \mathrm{U}(f(z_k))\right) \qquad s_\pm = \kappa_\pm \sigma_{SW}$$

- ❖ Estimate of σ_{SW} highly depends on the quality of the loss estimate
- ❖ These results have yet to be validated experimentally.

Statistical Behavior of Resonance Splitting (1)

- Multiplying energy rate equations by $i\hbar$ yields.

$$i\hbar\frac{d}{dt}\begin{bmatrix}a^+\\a^-\end{bmatrix} = \hbar\left(\gamma_t/2-\Delta\omega\right)\begin{bmatrix}1 & 0\\0 & 1\end{bmatrix}\begin{bmatrix}a^+\\a^-\end{bmatrix}$$

- Same form as TDSE and inherent adherence to requirements of said equation allow us to write.

$$\Psi \rightarrow \begin{bmatrix}a^+\\a^-\end{bmatrix} \qquad H^0 \rightarrow \hbar\left(\gamma_t/2-\Delta\omega\right)\begin{bmatrix}1 & 0\\0 & 1\end{bmatrix}$$

- Introducing contra-directional coupling

$$H = H^0 + H' = \hbar\left(\left(\gamma_t/2-\Delta\omega\right)\begin{bmatrix}1 & 0\\0 & 1\end{bmatrix} + \frac{\gamma_\beta}{2}\begin{bmatrix}0 & 1\\1 & 0\end{bmatrix}\right)$$

- Energy eigenvalues of E^c and E^s can be found

$$E^c = -\hbar\left(\gamma_t/2-\Delta\omega+\gamma_\beta/2\right) \quad \text{and} \quad E^s = -\hbar\left(\gamma_t/2-\Delta\omega-\gamma_\beta/2\right)$$

Statistical Behavior of Resonance Splitting (2)

- Our previous derivation shows that $\Delta\omega_{c,s} = \gamma_\beta$
- Via LLN, γ_β and, subsequently, $\Delta\omega_{c,s}$ follow a Rayleigh distribution.

$$p(\Delta\omega_{c,s}) = \frac{2\Delta\omega_{c,s}}{\langle\Delta\omega_{c,s}\rangle} exp\left(\frac{-\Delta\omega_{c,s}^2}{\langle\Delta\omega_{c,s}\rangle}\right)$$

- 418 resonances from eleven resonators fit
  - four port ring resonators with 50μm diameter and 400nm ring width
  - coupling gap and bus waveguide width varied

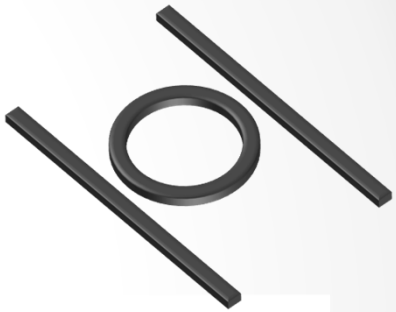

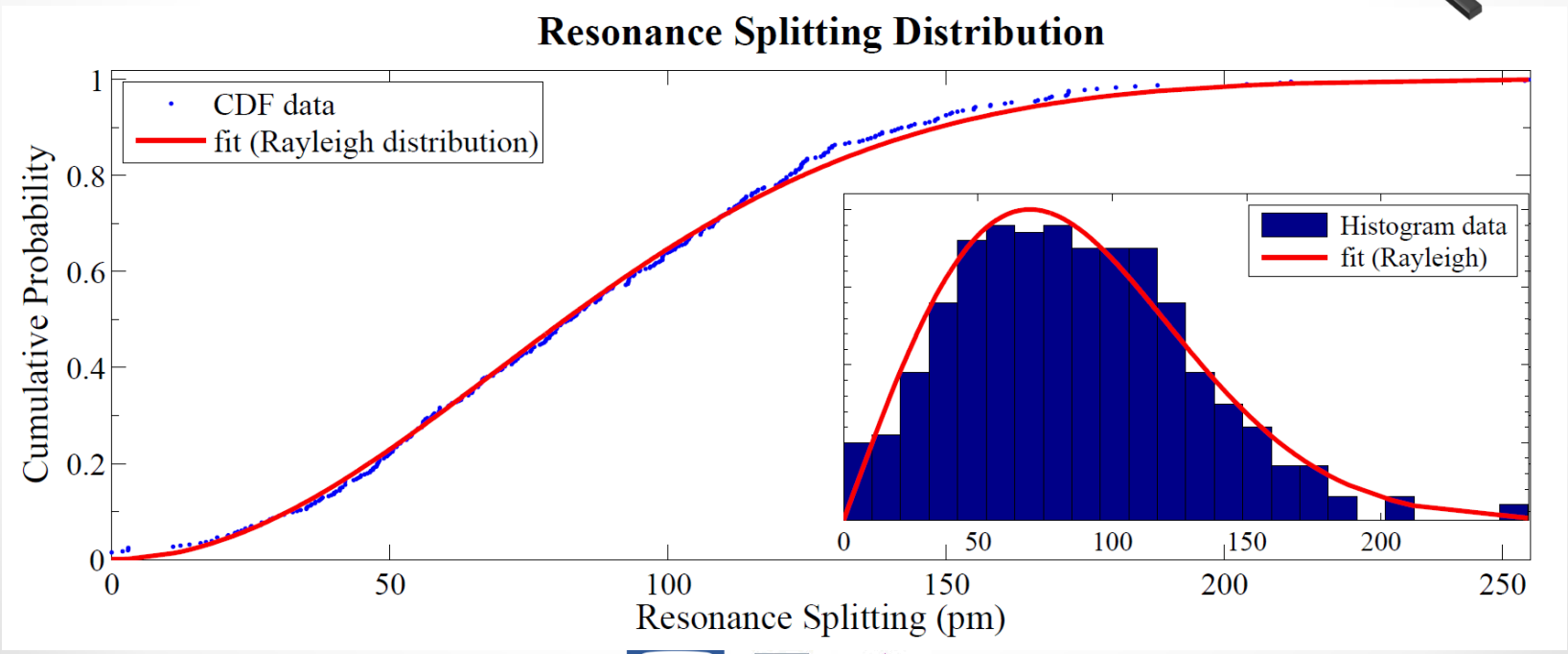

Scattering in Rough Waveguides & Resonators

Conclusions

- Scattering in rough waveguides caused loss and distributed contra-directional coupling.
- Reflected field of a passive waveguide can be represented as a random phasor sum.
- Transmitted measured intensity follows a smoothed Gamma distribution.
- A theoretical link between roughness size and transmitted intensity was derived but has yet to be experimentally validated.
- Resonance splitting caused by scattering induced contra-directional coupling follows a Rayleigh distribution.
- Theory dictates that very few resonances with zero splitting should be observed indicating that many doublets are incorrectly identified as singlet resonances.

Future Work

- Validate theoretical link between T' and σ_{SW}.
- Explore enhancement of contra-directional coupling via modification of scattering center geometry.
- Explore minimization of radiation mode coupling via modification of scattering center geometry.

Other Work

- Design of ring resonator based Optical Add/Drop Multiplexer (OADM).
- Study of curve fitting in the presence of speckle noise.
  - Heteroskedastic, correlated noise violates Gauss-Markov.
- Development of a loss envelope removal algorithm utilizing morphological erosion.
- Development of a noise-robust resonance locating algorithm.
- Development of a perturbative approach to split resonance fitting.
  - Reduce six parameter fit with a large number of local minima in the 6D error function to a series of three parameter fits with a single global minima.

Acknowledgements

- University of Arizona, College of Optical Sciences
- Sandia National Labs, Org. 1765 Applied Photonic Microsystems

Questions